Article

Novel Aromatic Poly(Amine-Imide)s Bearing A Pendent Triphenylamine Group: Synthesis, Thermal, Photophysical, Electrochemical, and Electrochromic Characteristics

Shu-Hua Cheng, Sheng-Huei Hsiao, Tzy-Hsiang Su, and Guey-Sheng Liou

Macromolecules, **2005**, 38 (2), 307-316 • DOI: 10.1021/ma048774d

Novel Aromatic Poly(Amine-Imide)s Bearing A Pendent Triphenylamine Group: Synthesis, Thermal, Photophysical, Electrochemical, and Electrochromic Characteristics

Shu-Hua Cheng,[†] Sheng-Huei Hsiao,[‡] Tzy-Hsiang Su,[†] and Guey-Sheng Liou*,[†]

Department of Applied Chemistry, National Chi Nan University, 1 University Road, Nantou Hsien 545, Taiwan, Republic of China, and Department of Chemical Engineering, Tatung University, 40 Chungshan North Rd. 3rd Sec., Taipei 104, Taiwan, Republic of China

Received June 21, 2004; Revised Manuscript Received October 23, 2004

ABSTRACT: A new triphenylamine-containing aromatic diamine, *N*,*N*-bis(4-aminophenyl)-*N*′,*N*′-diphenyl-1,4-phenylenediamine, was synthesized from the amination reaction between 4-aminotriphenylamine and 4-fluoronitrobenzene and subsequent reduction of the dinitro intermediate. A series of novel aromatic poly(amine-imide)s with pendent triphenylamine units were prepared from the newly synthesized diamine and various tetracarboxylic dianhydrides by either a one-step or a conventional two-step polymerization process. All the poly(amine-imide)s were amorphous and readily soluble in many organic solvents such as *N*-methyl-2-pyrrolidone (NMP), *N*,*N*-dimethylacetamide, and chloroform. These polymers could be solution cast into transparent, tough, and flexible films with good mechanical properties. They had useful levels of thermal stability associated with relatively high glass transition temperatures (264−352 °C), 10% weight-loss temperatures in excess of 568 °C, and char yields at 800 °C in nitrogen higher than 63%. These polymers exhibited strong UV−vis absorption bands at 311−330 nm in NMP solution. The photoluminescence spectra showed maximum bands around 545−562 nm in the green region. The hole-transporting and electrochromic properties are examined by electrochemical and spectroelectrochemical methods. Cyclic voltammograms of the poly(amine-imide) films cast onto an indium−tin oxide (ITO)-coated glass substrate exhibited two reversible oxidation redox couples at 0.78 and 1.14 V versus Ag/AgCl in acetonitrile solution. The poly(amine-imide) films revealed excellent stability of electrochromic characteristics, with a color change from the pale yellowish neutral form to the green and blue oxidized forms at applied potentials ranging from 0.78 to 1.14 V.

Introduction

Semiconducting, conducting, and light-emitting organic materials are showing increasing potential as active components for a wide range of electronic and optoelectronic devices. Arylamine-containing aromatics have been used as hole-transporting molecules in the optoelectronic fields, both in photoreceptor devices[1] and organic light emitting diodes (OLEDs).[2,3] The redox properties, ion transfer process, electrochromism, and photoelectrochemical behavior of *N*,*N*,*N*′,*N*′-tetrasubstituted-1,4-phenylenediamines are of importance for technological application.[4−7] A new material with longer life, higher efficiency, and appropriate HOMO energy level is in increasing demand. In recent years, intensive research efforts have been focused on the development of new charge-transport polymers since they promise a number of commercial advantages over low-molecular-weight counterparts.[8] One of the perceived advantages is that polymer films can be more easily deposited over a larger area and they are often flexible. Furthermore, prevention of crystallization and phase-separation may improve the device performance. Since triarylamine derivatives have been widely used as hole-transport compounds in organic photoconductors and electroluminescent devices,[9−15] many triarylamine macromolecules have been developed, and some important results have been obtained.[16−24]

Aromatic polyimides are well accepted as advanced materials for a thin-film application in microelectronic devices and liquid crystal displays due to their outstanding mechanical, chemical, thermal, and physical properties.[25,26] However, the technological applications of most polyimides are limited by processing difficulties because of high melting or glass transition temperatures (T_g's) and limited solubility in most organic solvents. To overcome such a difficulty, polymer-structure modification becomes necessary. One of the common approaches for increasing solubility and processability of polyimides without sacrificing high thermal stability is the introduction of bulky, packing-disruptive groups into the polymer backbone.[27−34] Recently, we have reported the synthesis of soluble aromatic polyamides and polyimides bearing triphenylamine units in the main chain based on *N*,*N*′-bis(4-aminophenyl)-*N*,*N*′-diphenyl-1,4-phenylenediamine,[35,36] *N*,*N*′-bis(4-carboxyphenyl)-*N*,*N*′-diphenyl-1,4-phenylenediamine,[37] and 2,4-diaminotriphenylamine,[38] respectively. Because of the incorporation of bulky, three-dimensional triphenylamine units along the polymer backbone, all the polymers were amorphous, had good solubility in many aprotic solvents, and exhibited excellent thin-film-forming capability.

In the present article, we report the synthesis of a series of novel poly(amine-imide)s bearing pendent triphenylamine groups based on a new diamine, *N*,*N*-bis(4-aminophenyl)-*N*′,*N*′-diphenyl-1,4-phenylenediamine (**4**). The general properties such as solubility, crystallinity, and thermal and mechanical properties are reported. The electrochemical, electrochromic, and photoluminescence properties of these polymers prepared

* Author to whom correspondence should be addressed. E-mail: gsliou@ncnu.edu.tw.
[†] National Chi Nan University.
[‡] Tatung University.

10.1021/ma048774d CCC: $30.25
Published on Web 12/22/2004

by casting solution onto an indium−tin oxide (ITO)-coated glass substrate are also described herein and are compared with those of structurally related ones from 4,4′-diaminotriphenylamine.

Experimental Section

Materials. 4,4′-Diaminotriphenylamine (mp = 186−187 °C) was synthesized by hydrazine Pd/C-catalyzed reduction of 4,4′-dinitrotriphenylamine resulting from the cesium fluoride-assisted condensation of aniline with 4-fluoronitrobenzene according to a reported procedure.[39] Commercially available aromatic tetracarboxylic dianhydrides such as pyromellitic dianhydride (PMDA) (**5a**) (Chriskev), 3,3′,4,4′-benzophenonetetracarboxylic dianhydride (BTDA) (**5c**) (Chriskev), 4,4′-oxydiphthalic dianhydride (ODPA) (**5d**) (TCI), and 3,3′,4,4′-diphenylsulfonetetracarboxylic dianhydride (DSDA) (**5e**) (TCI) were purified by recrystallization from acetic anhydride. 3,3′,4,4′-Biphenyltetracarboxylic dianhydride (BPDA) (**5b**) (Chriskev) and 2,2-bis(3,4-dicarboxyphenyl)hexafluoropropane dianhydride (6FDA) (**5f**) (Chriskev) were purified by vacuum sublimation. Tetrabutylammonium perchlorate (TBAP) was obtained from Acros and recrystallized twice from ethyl acetate and then dried in vacuo prior to use. All other reagents were used as received from commercial sources.

Monomer Synthesis. *4-Nitrotriphenylamine (**1**) and 4-Aminotriphenylamine (**2**).* According to well-known chemistry,[40,41] compound **1** (mp = 144−145 °C; lit.[42] 141.5−142 °C) was prepared by the aromatic nucleophilic amination of 4-nitrofluorobenzene and diphenylamine in *N,N*-dimethylformamide (DMF) in the presence of sodium hydride. Subsequent reduction of **1** by means of hydrazine and Pd/C in refluxing ethanol gave compound **2** (mp = 148−149 °C). The molecular structures of **1** and **2** were confirmed by elemental, IR, ^{1}H NMR, and ^{13}C NMR analyses.

*N,N-Bis(4-nitrophenyl)-N′,N′-diphenyl-1,4-phenylenediamine (**3**).* A mixture of 1.77 g (0.070 mol) of sodium hydride and 100 mL of DMF was stirred at room temperature. To the mixture, 9.11 g (0.035 mol) of compound **2** and 10.12 g (0.071 mol) of 4-fluoronitrobenzene were added in sequence. The mixture was heated with stirring at 110 °C for 15 h and then precipitated into 700 mL of methanol. Recrystallization from acetonitrile yielded 8.46 g of the desired dinitro compound **3** as dark red crystals in 48% yield; mp = 219−220 °C measured by DSC at 2 °C/min. IR (KBr): 1578, 1303 cm^{-1} (−NO_2 stretch). ^{1}H NMR (DMSO-d_6, ppm): 8.20 (d, J = 9.1 Hz, 4H, H_g), 7.36 (t, J = 8.1 Hz, 4H, H_d), 7.24 (d, J = 9.1 Hz, 4H, H_f), 7.15 (d, J = 8.8 Hz, 2H, H_b), 7.11 (t, J = 7.9 Hz, 2H, H_e), 7.10 (d, J = 7.9 Hz, 4H, H_c), 7.02 (d, J = 8.8 Hz, 2H, H_a). ^{13}C NMR (DMSO-d_6, ppm): 151.9 (C^9), 147.0 (C^5), 146.4 (C^4), 142.1 (C^{12}), 138.1 (C^1), 130.0 (C^7), 128.8 (C^3), 125.8 (C^{10}), 124.8 (C^6), 124.0 (C^8), 123.8 (C^2), 122.3 (C^{11}). Anal. Calcd for $C_{30}H_{22}N_4O_4$ (502.52): C, 71.70%; H, 4.41%; N, 11.15%. Found: C, 71.41%; H, 4.40%; N, 11.02%. Crystal data: Dark red crystal grown during the slow crystallization in acetonitrile, 0.35 × 0.25 × 0.20 mm^3, Triclinic P*1* with a = 11.1490(3), b = 11.4860(3), c = 11.6470(3) Å; α = 70.2780(10)°, β = 63.958(2)°, γ = 73.576(2)°, where the density of crystal Dc = 1.340 Mg/m^3 for Z = 2 and V = 1245.38(6) Å^3.

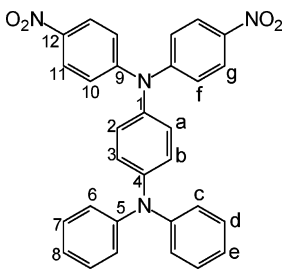

*N,N-Bis(4-aminophenyl)-N′,N′-diphenyl-1,4-phenylenediamine (**4**).* In a 500-mL round-bottom flask equipped with a stirring bar, a mixture of 8.88 g (0.018mol) of dinitro compound **3,** 0.2 g of 10% Pd/C, 5 mL of hydrazine monohydrate, and 150 mL of ethanol was heated at reflux for 10 h. After being cooled to room temperature, 150 mL of tetrahydrofuran (THF) was added to dissolve the precipitate. The solution was filtered to remove Pd/C catalyst, and the filtrate was distilled to remove the solvent. The crude product was washed with methanol and recrystallized from toluene in nitrogen and dried in vacuo at 100 °C to give 7.02 g (yield: 89%) of light-beige product; mp = 245−247 °C measured by DSC at 2 °C/min. IR (KBr): 3368, 3457 cm^{-1} (N−H stretch). ^{1}H NMR (DMSO-d_6, ppm): 7.21 (t, J = 7.7 Hz, 4H, H_d), 6.92 (d, J = 7.3 Hz, 4H, H_c), 6.91 (t, J = 7.5 Hz, 2H, H_e), 6.84 (d, J = 8.6 Hz, 4H, H_f), 6.82 (d, J = 8.9 Hz, 2H, H_b), 6.60 (d, J = 8.9 Hz, 2H, H_a), 6.57 (d, J = 8.6 Hz, 4H, H_g), 4.95 (s, 4H, −NH_2). ^{13}C NMR (DMSO-d_6, ppm): 147.9 (C^5), 146.7 (C^4), 145.6 (C^{12}), 137.4 (C^1), 136.4 (C^9), 129.4 (C^7), 127.4 (C^{10}), 127.2 (C^3), 122.2 (C^6), 121.8 (C^8), 118.0 (C^2), 115.2 (C^{11}). Anal. Calcd for $C_{30}H_{26}N_4$ (442.55): C, 81.42%; H, 5.92%; N, 12.66%. Found: C, 81.14%; H, 6.01%; N, 12.42%.

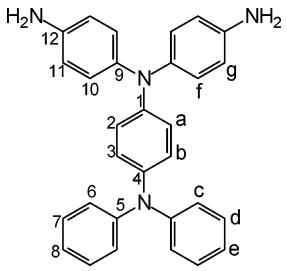

Polymer Synthesis. *Poly(Amine-Imide) **6a** by a Two-Step Method via Thermal Imidization Reaction.* The diamine monomer **4** (0.6699 g, 1.514 mmol) was dissolved in 10 mL of DMAc in a 50-mL round-bottom flask. Then, PMDA (0.3302 g, 1.514 mmol) was added to the diamine solution in one portion. Thus, the solid content of the solution is approximately 10 wt%. The mixture was stirred at room temperature for about 4 h to yield a viscous polyamic acid solution. The inherent viscosity of the resulting polyamic acid was 0.82 dL/g, measured in DMAc at a concentration of 0.5 g/dL at 30 °C. The polyamic acid film was obtained by casting from the reaction polymer solution onto a glass plate and drying at 90 °C overnight under vacuum. The polyamic acid in the form of film was converted to poly(amine-imide) **6a** by successive heating under vacuum at 100 °C for 1 h, 200 °C for 1 h, and then 300 °C for 1 h. The inherent viscosity of poly(amine-imide) **6a** was 0.34 dL/g, measured at a concentration of 0.5 g/dL in concentrated sulfuric acid at 30 °C. Anal. Calcd for $(C_{40}H_{24}N_4O_4)_n$ (624.64)$_n$: C, 76.91%; H, 3.87%; N, 8.97%. Found: C, 76.24%; H, 4.05%; N, 8.93%. The other poly(amine-imide)s **6b**−**6f** were prepared by the one-step method.

*Poly(Amine-Imide)s **6b**−**6f** by a One-Step Method.* A typical procedure is as follows. A stoichiometric mixture of diamine **4** (0.6638 g, 1.5 mmol) and dianhydride **5d** (0.4654 g, 1.5 mmol) and a few drops of isoquinoline in *m*-cresol (10 mL) were stirred at ambient temperature under nitrogen. After the solution was stirred for 5 h, it was heated to 200 °C and maintained at that temperature for 15 h. After the solution was allowed to cool to ambient temperature, the viscous solution then was poured slowly into 300 mL of methanol with stirring. The polymer that precipitated was collected by filtration, washed thoroughly with hot methanol, and dried at 150 °C for 15 h in vacuo. Precipitations from NMP into methanol were carried out twice for further purification. The poly(amine-imide) **6d** was obtained having inherent viscosity of 0.36 dL/g, measured at a concentration of 0.5 g/dL in NMP at 30 °C. The IR spectrum of **6d** (film) exhibited characteristic imide absorption bands at 1775 (asymmetrical C−O), 1721 (symmetrical C−O), 1377 (C−N), and 739 cm^{-1} (imide ring deformation). Anal. Calcd for $(C_{46}H_{28}N_4O_5)_n$ (716.74)$_n$: C, 77.08%; H, 3.94%; N, 7.82%. Found: C, 76.43%; H, 4.01%; N, 7.62%. Poly(amine-imide)s **6b**−**6f** were prepared by an analogous procedure.

Scheme 1

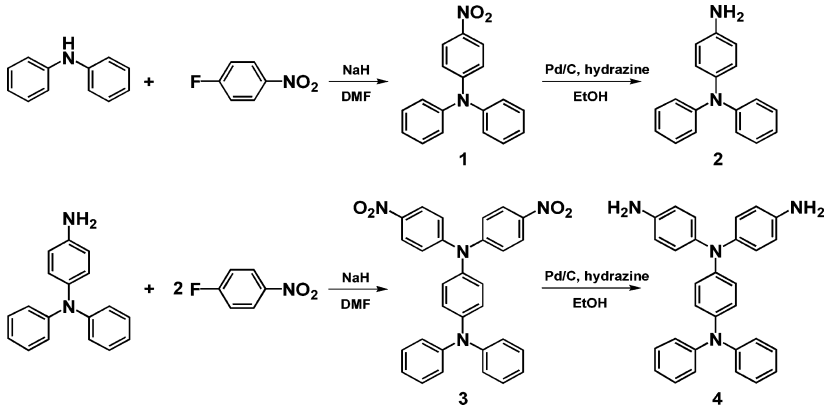

Film Preparation. A polymer solution was made by the dissolution of about 0.7 g of the poly(amine-imide) sample in 10 mL of NMP. The homogeneous solution was poured into a 9-cm glass Petri dish, which was placed in a 90 °C oven overnight for the slow release of the solvent, and then the film was stripped off from the glass substrate and further dried in vacuo at 180 °C for 8 h. The obtained films were about 60−80 μm thick and were used for X-ray diffraction measurements, tensile tests, solubility tests, and thermal analyses.

Measurements. Infrared spectra were recorded on a PerkinElmer RXI FT-IR spectrometer. Elemental analyses were run in an Elementar VarioEL-III. ^{1}H and ^{13}C NMR spectra were measured on a Bruker Avance 500 MHz FT-NMR system. The inherent viscosities were determined at a 0.5 g/dL concentration using an Tamson TV-2000 viscometer at 30 °C. Wide-angle X-ray diffraction (WAXD) measurements were performed at room temperature (ca. 25 °C) on a Shimadzu XRD-7000 X-ray diffractometer (40 kV, 20 mA), using graphite-monochromatized Cu Kα radiation. UV−vis spectra of the polymer films were recorded on a Varian Cary 50 probe spectrometer. An Instron universal tester model 4400R with a load cell of 5 kg was used to study the stress−strain behavior of the samples. A gauge length of 2 cm and a crosshead speed of 5 mm/min were used for this study. Measurements were performed at room temperature with film specimens (0.5 cm width, 6 cm length), and an average of at least three replicates was used. Thermogravimentric analysis (TGA) was conducted with a PerkinElmer Pyris 1 TGA. Experiments were carried out on approximately 6−8-mg film samples heated in flowing nitrogen or air (flow rate = 20 cm^3/min) at a heating rate of 20 °C/min. DSC analyses were performed on a PerkinElmer Pyris Diamond DSC at a scan rate of 20 °C/min in flowing nitrogen (20 cm^3/min). Thermomechanical analysis (TMA) was conducted with a PerkinElmer TMA 7 instrument. The TMA experiments were conducted from 50 to 350 °C at a scan rate of 10 °C/min with a penetration probe 1.0 mm in diameter under an applied constant load of 10 mN. Softening temperatures (T_s) were taken as the onset temperatures of probe displacement on the TMA traces. Electrochemistry was performed with a Bioanalytical System Model CV-27 potentiostat and a BAS *X*−*Y* recorder. Voltammograms are presented with the positive potential pointing to the left and with increasing anodic currents pointing downward. Cyclic voltammetry was conducted with the use of a three-electrode cell in which ITO (polymer films area about 0.7 × 0.5 cm^2) was used as a working electrode. A platinum wire was used as an auxiliary electrode. All cell potentials were taken with the use of a homemade Ag/AgCl, KCl (sat.) reference electrode. The spectroelectrochemical cell was composed of a 1-cm cuvette, ITO as a working electrode, a platinum wire as an auxiliary electrode, and a Ag/AgCl reference electrode. Absorption spectra were measured with a HP 8453 UV−vis spectrophotometer. Photoluminescence spectra were measured with a Jasco FP-6300 spectrofluorometer.

Results and Discussion

Monomer Synthesis. 4-Aminotriphenylamine (**2**) was prepared by the condensation of diphenylamine with 4-fluoronitrobenzene followed by hydrazine Pd/C-catalytic reduction according to the synthetic route outlined in Scheme 1. The new aromatic diamine having a bulky pendent triphenylamine group, *N*,*N*-bis(4-aminophenyl)-*N*′,*N*′-diphenyl-1,4-phenylenediamine (**4**), was successfully synthesized by the amination reaction of **2** with 4-fluoronitrobenzene followed by hydrazine Pd/C-catalytic reduction. Elemental analysis, IR, and ^{1}H and ^{13}C NMR spectroscopic techniques were used to identify the structures of the intermediate compounds **1**, **2**, and **3** and the diamine monomer **4**. The transformation of nitro to amino functionality could be monitored by the change of IR spectra. The nitro groups of compounds **1** and **3** gave two characteristic bands at around 1580 and 1313 cm^{-1} ($-NO_2$ asymmetric and symmetric stretching). After reduction, the characteristic absorptions of the nitro group disappeared and the amino group showed the typical N−H stretching absorption pair in the region of 3300−3500 cm^{-1}. Figure 1 illustrates the ^{1}H NMR and ^{13}C NMR spectra of the diamine monomer **4.** Assignments of each carbon and proton are assisted by the two-dimensional NMR spectra shown in Figures 2 and 3, and these spectra agree well with the proposed molecular structure of **4**. The ^{1}H NMR spectra confirm that the nitro groups have been completely transformed into amino groups by the high-field shift of the aromatic protons and by the resonance signals at around 5.0 ppm corresponding to

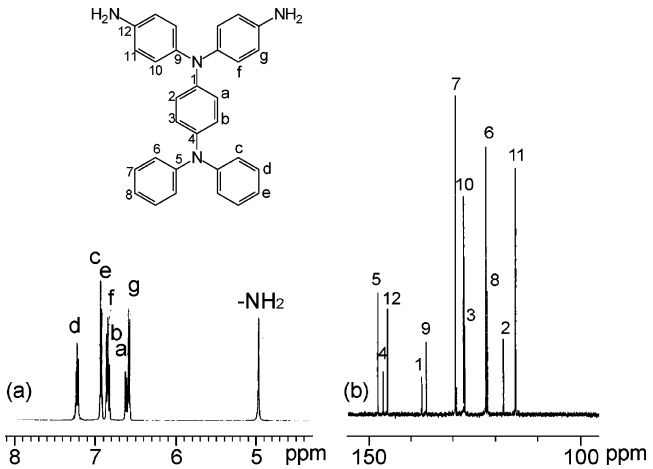

Figure 1. (a) ^{1}H NMR and (b) ^{13}C NMR spectra of diamine monomer **4** in DMSO-d_6.

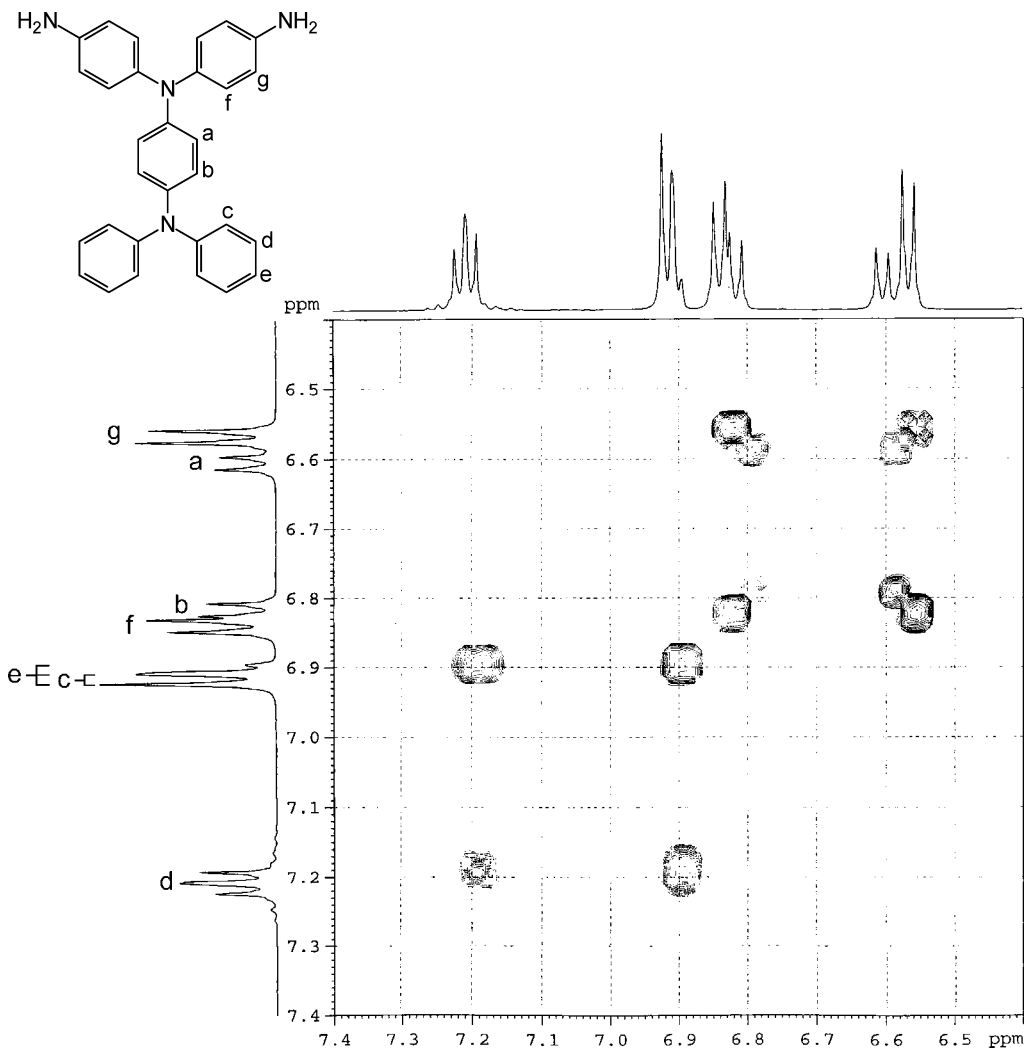

Figure 2. H−H COSY spectrum of diamine monomer **4** in DMSO-d_6.

the amino protons. The molecular structure of dinitro compound **3** was also confirmed by X-ray crystal analysis acquired from the single crystal obtained by slow crystallization of an acetonitrile solution of **3**. As shown in Figure 4, the dinitro compound **3** displays a propeller-shaped configuration of the triphenylamine cores and the benzene rings are not in the same plane. This conformation will hinder the close packing of polymer chains and enhance the solubility of formed poly(amine-imide)s.

Polymer Synthesis. The one-step procedure starting from aromatic diamines and tetracarboxylic dianhydrides in the presence of isoquinoline as a catalyst, as well as conventional two-step process, involving a ring-opening addition and subsequent thermal cyclodehydration, are convenient methods for the preparation of polyimides.[25] New poly(amine-imide)s **6b**−**6f** were synthesized by the one-step method starting from diamine monomer **4** with aromatic tetracarboxylic dianhydrides **5b**−**5f** in the presence of a catalytic amount of isoquinoline in refluxing *m*-cresol (Scheme 2). Due to less solubility, poly(amine-imide) **6a** was prepared by the conventional two-step method via thermal imidization reaction. The formation of poly(amine-imide)s was confirmed with elemental analysis, IR spectroscopy, and NMR spectroscopy. The results of elemental analysis shown in Table 1 supported the formation of the expected polymers. The IR spectra of these polymers exhibited characteristic imide absorption bands at around 1775 (asymmetrical C−O), 1720 (symmetrical C−O), 1380 (C_N), and 740 cm^{-1} (imide ring deformation). The microstructures of these poly(amine-imide)s were also verified by the high-resolution NMR spectra. For a comparative study, a series of referenced poly(amine-imide)s **6a′**−**6f′** were also synthesized from 4,4′-diaminotriphenylamine and dianhydrides **5a**−**5f**.

Basic Characterization. The X-ray diffraction studies of the poly(amine-imide)s indicated that all the polymers were essentially amorphous. The qualitative solubility properties of polymers **6a**−**6f** are reported in Table 2. On comparing with the corresponding poly(amine-imide)s **6′**, the present series of poly(amine-imide)s exhibited an enhanced solubility because of the increased flexibility or free volume caused by the introduction of a bulky pendent triphenylamine group in the repeat unit. The excellent solubility makes these poly(amine-imide)s potential candidates for practical applications in spin- or dip-coating processes.

All the aromatic poly(amine-imide)s could afford flexible and tough films. These films were subjected to tensile testing, and the results are given in Table 3. The tensile strengths, elongations to break, and initial moduli of these films were in the ranges of 87−119 MPa, 8−12%, and 2.0−2.6 GPa, respectively.

The thermal properties of the poly(amine-imide)s were investigated by TGA, DSC, and TMA. The results

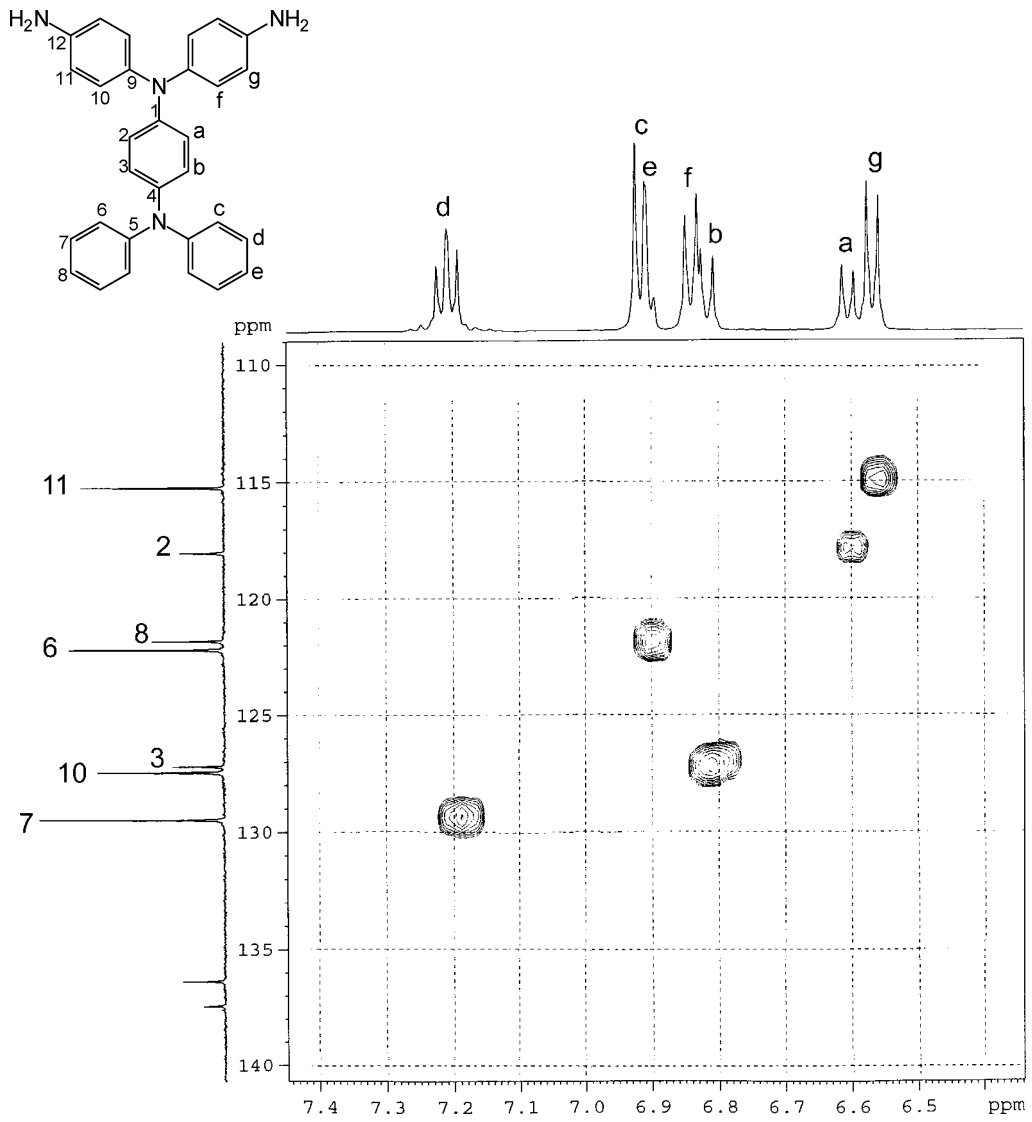

Figure 3. C−H COSY spectrum of diamine monomer **4** in DMSO-d_6.

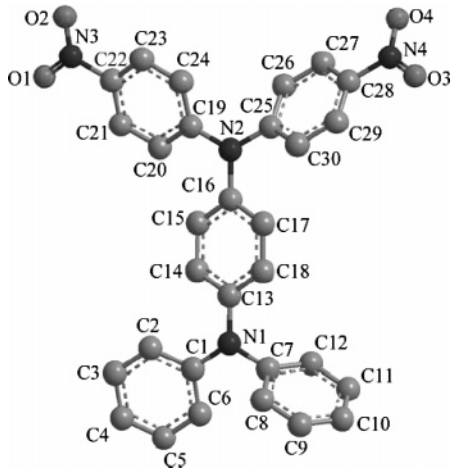

Figure 4. Molecular structure of dinitro compound **3** by single-crystal X-ray analysis.

are summarized in Table 4. Typical TGA curves for poly(amine-imide) **6e** are reproduced in Figure 5. All of the poly(amine-imide)s exhibited a similar TGA pattern with no significant weight loss below 500 °C both in air and in nitrogen atmosphere. The 10% weight-loss temperatures of the poly(amine-imide)s in nitrogen and air were recorded in the range of 568−629 and 574−622 °C, respectively. The amount of carbonized residue (char yield) of these polymers in nitrogen atmosphere was more than 63% at 800 °C. The high char yields of these polymers can be ascribed to their high aromatic content. This outstanding thermal stability also renders advantages in various applications. The glass-transition temperatures (T_g) of all the polymers were observed in the range of 264−352 °C by DSC and decreased with decreasing rigidity of the tetracarboxylic dianhydride used. When compared with the analogous poly(amine-imide)s **6′**, the **6** series of poly(amine-imide)s showed a slightly decreased T_g that may be attributed to the increased conformational flexibility or free volume caused by the introduction of the bulky pendent triphenylamine group in the repeat unit. These results are consistent with those reported previously.[35−37] All the polymers indicated no clear melting endotherms up to the decomposition temperatures on the DSC thermograms. This result also supports the amorphous nature of these triphenylamine-containing polymers. The softening temperatures (T_s) of the polymer film samples were determined by the TMA method with a loaded penetration probe. They were obtained from the onset temperature of the probe displacement on the TMA trace. A typical TMA thermogram for poly(amine-imide) **6d** is illustrated in Figure 6. There is a large window

Scheme 2. Synthesis of Poly(amine-imide)s by the One-step Method

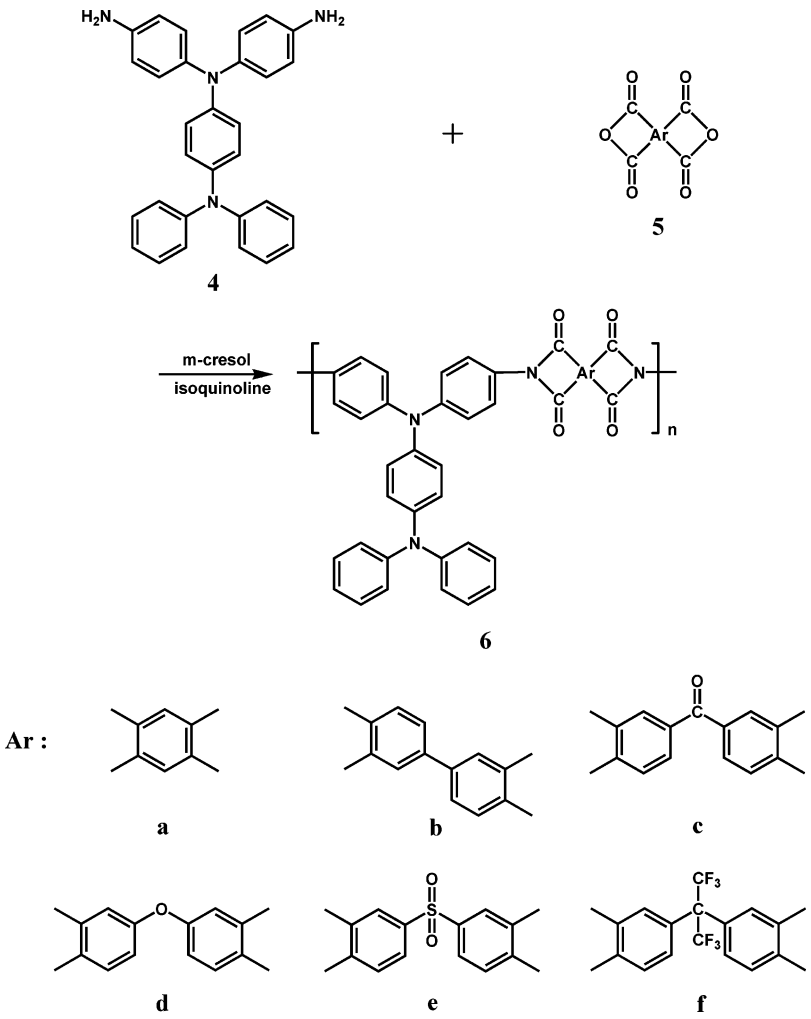

Table 1. Inherent Viscosity and Elemental Analysis of Poly(Amine-Imide)s

poly(amine-imide)s		elemental analysis (%) of poly(amine-imide)s					
code	η_{inh}[a] (dL/g)	formula (formula weight)		C	H	N	S
6a	0.34	$(C_{40}H_{24}N_4O_4)_n$	calcd	76.91	3.87	8.97	
		$(624.64)_n$	found	76.24	4.05	8.93	
6b	0.39	$(C_{46}H_{28}N_4O_4)_n$	calcd	78.84	4.03	8.00	
		$(700.74)_n$	found	77.67	4.12	7.81	
6c	0.35	$(C_{47}H_{28}N_4O_5)_n$	calcd	77.46	3.87	7.69	
		$(728.75)_n$	found	76.86	4.04	7.41	
6d	0.36	$(C_{46}H_{28}N_4O_5)_n$	calcd	77.08	3.94	7.82	
		$(716.74)_n$	found	76.43	4.01	7.62	
6e	0.32	$(C_{46}H_{28}N_4O_6S)_n$	calcd	72.24	3.69	7.33	4.19
		$(764.80)_n$	found	71.51	3.88	7.10	4.07
6f	0.29	$(C_{49}H_{28}F_6N_4O_4)_n$	calcd	69.18	3.32	6.59	
		$(850.76)_n$	found	68.73	3.43	6.32	

[a] Measured at a polymer concentration of 0.5 g/dL in NMP at 30 °C (**6a** and **6b**: measured in concentrated sulfuric acid).

between T_g or T_s and the decomposition temperature of each polymer, which could be advantageous in the processing of these polymers by the thermoforming technique.

Optical and Electrochemical Properties. The optical and electrochemical properties of the poly(amine-imide)s were investigated by cyclic voltammetry, UV−vis spectroscopy, and photoluminescence spectroscopy. The results are summarized in Table 5. These polymers (**6b**−**6f**) exhibited strong UV−vis absorption bands at 311−330 nm in NMP solution, assignable to the $\pi-\pi^*$ transition resulting from the conjugation between the aromatic rings and nitrogen atoms. Their photoluminescence spectra in NMP solution showed maximum bands around 545−562 nm in the green region. Figure 7 shows UV−vis absorption and photoluminescence spectra of poly(amine-imide)s **6d, 6e, 6′d**, and **6′e** for comparison. These polymers exhibited similar spectrograms while the PL intensity of the poly(amine-imide)s **6′** series is greater than that of the poly(amine-imide)s **6** series. This phenomenon possibly could be attributed to the fact that the excited-state energy of the **6** series is more likely released in a vibrational way because of the greater conformational mobility. The cutoff wave-

Table 2. Solubility of Aromatic Poly(Amine-Imide)s

	solvents[a]						
polymer	NMP	DMAc	DMF	DMSO	*m*-cresol	THF	chloroform
6a	+h (−)[b]	± (−)	± (−)	± (−)	+h (−)	− (−)	± (−)
6b	+h (+h)	± (−)	± (−)	± (−)	+h (−)	± (+h)	+ (−)
6c	+ (+h)	+ (+h)	+ (+h)	+h (+h)	+ (+h)	+ (−)	+ (−)
6d	+ (+h)	+ (+h)	± (−)	+h (+h)	+h (+h)	± (−)	+ (−)
6e	+ (+h)	+ (−)	+ (−)	+h (+h)	+h (+h)	+ (−)	+ (−)
6f	+ (−)	+ (−)	+ (−)	+h (+h)	+h (+h)	+ (−)	+ (−)

[a] Solubility: +, soluble at room temperature; +h, soluble on heating; ±, partially soluble or swelling; −, insoluble even on heating. [b] Data in parentheses are the solubility of analogous poly(amine-imide)s (**6′**) having the corresponding dianhydride residue as in the **6** series.

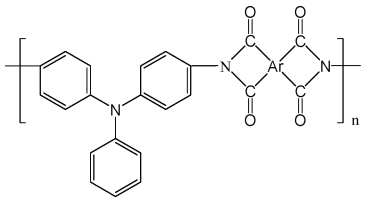

6'

Table 3. Mechanical Properties of Poly(Amine-Imide) Films

polymer	tensile strength (MPa)	elongation at break (%)	initial modulus (GPa)
6a	87	10	2.1
6b	119	12	2.3
6c	102	8	2.6
6d	101	11	2.0
6e	111	9	2.3
6f	95	9	2.2

lengths (absorption edge; λ_0) from the UV−vis absorption spectra are also included in Table 5. It revealed that most of the visible region can be absorbed by poly(amine-imide)s **6a** and **6e** which show higher λ_0 values. This is consistent with the fact that the films of polymers **6a** and **6c** appeared deep red-brown color. The redox behavior was investigated with cyclic voltammetry conducted for the cast film on an ITO-coated glass substrate as working electrode in dry acetonitrile (CH_3CN) containing 0.1 M TBAP as an electrolyte under nitrogen atmosphere. The typical cyclic voltammograms for poly(amine-imide)s **6e** and **6′e** are shown in Figure 8. There are two reversible oxidation redox couples at $E_{1/2}$ = 0.78 and 1.14 V, respectively, for poly(amine-imide) **6e** and one reversible oxidation redox couple at $E_{1/2}$ = 1.08 V for poly(amine-imide) **6′e** in the oxidative scan. Because of the stability of the films and the good adhesion between the polymer and ITO substrate, the poly(amine-imide) **6e** exhibited excellent reversibility of electrochromic characteristics by five continuous cyclic scans between 0.0 and 1.35 V, changing color from pale yellowish to green then blue at electrode potentials ranging from 0.78 to 1.14 V. Comparing the electrochemical data, it was found that poly(amine-imide) **6e** is much more easily oxidized than poly(amine-imide) **6′e** (0.78 vs 1.08 V). The first electron removal for poly(amine-imide) **6e** is assumed to occur at the nitrogen atom on the pendent triphenyl unit, which is more electron-rich than the nitrogen atom on the main-chain triphenylamine group. The energy of the HOMO and LUMO levels of the investigated poly(amine-imide)s can be determined from the oxidation half-wave potentials

Table 4. Thermal Properties of Aromatic Poly(Amine-Imide)s

			T_d at 5% weight loss (°C)[c]		T_d at 10% weight loss (°C)[c]		char yield
polymer	T_g (°C)[a]	T_s (°C)[b]	N_2	air	N_2	air	(wt%)[d]
6a	352 (−)	327 (314)	607	584	624 (606)	610 (596)	68 (70)
6b	302 (331)[e]	267 (314)	602	591	629 (613)	622 (619)	70 (68)
6c	294 (309)	251 (290)	582	537	618 (590)	589 (590)	63 (67)
6d	264 (295)	258 (292)	586	567	610 (608)	600 (611)	74 (66)
6e	305 (326)	281 (291)	528	537	568 (546)	582 (577)	67 (60)
6f	286 (316)	261 (310)	559	546	585 (581)	574 (571)	68 (63)

[a] Midpoint temperature of baseline shift on the second DSC heating trace (rate 20 °C/min) of the sample after quenching from 400 °C. [b] Softening temperature measured by TMA with a constant applied load of 10 mN at a heating rate of 10 °C/min. [c] Decomposition temperature, recorded via TGA at a heating rate of 20 °C/min and a gas-flow rate of 30 cm^3/min. [d] Residual weight percentage at 800 °C in nitrogen. [e] Values in parentheses are data of analogous poly(amine-imide)s (**6′**) having the corresponding dianhydride residue as in the **6** series.

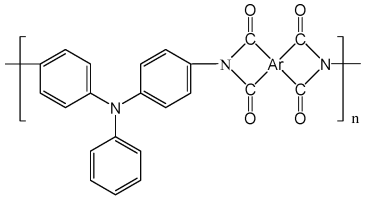

6'

Table 5. Optical and Electrochemical Properties of the Aromatic Poly(Amine-Imide)s

code	$\lambda_{abs,\ max}$ (nm)[a]	$\lambda_{abs,\ onset}$ (nm)[a]	λ_{PL} (nm)[b]	λ_0 (nm)[c]	oxidation (V) (vs Ag/AgCl) first	oxidation (V) (vs Ag/AgCl) second	HOMO−LUMO gap[d] (eV)	HOMO[e] (eV)	LUMO[f] (eV)
6a[g]	–	–	–	661	–	–	–	–	–
6b	330	387	562	577	0.78	1.14	3.20	5.08	1.88
6c	316	388	555	588	0.78	1.13	3.20	5.08	1.88
6d	324	385	545	499	0.78	1.13	3.22	5.08	1.86
6e	311	390	556	608	0.79	1.14	3.18	5.09	1.91
6f	326	385	546	508	0.80	1.14	3.22	5.10	1.88
6′d	314	378	534	456	1.06	–	3.28	5.36	2.08
6′e	304	385	547	549	1.08	–	3.22	5.38	2.16

[a] UV−vis absorption measurements in NMP (0.02 mg/mL) at room temperature. [b] PL spectra measurements in NMP (5 mg/mL) at room temperature. [c] The cutoff wavelengths (λ_0) from the transmission UV−vis absorption spectra of polymer films. [d] The data were calculated by the equation: gap = $1240/\lambda_{onset}$. [e] The HOMO energy levels were calculated from cyclic voltammetry and were referenced to ferrocene (4.8 eV). [f] LUMO = HOMO − gap. [g] Poly(amine-imide) **6a** is difficult to dissolve into the NMP solvent.

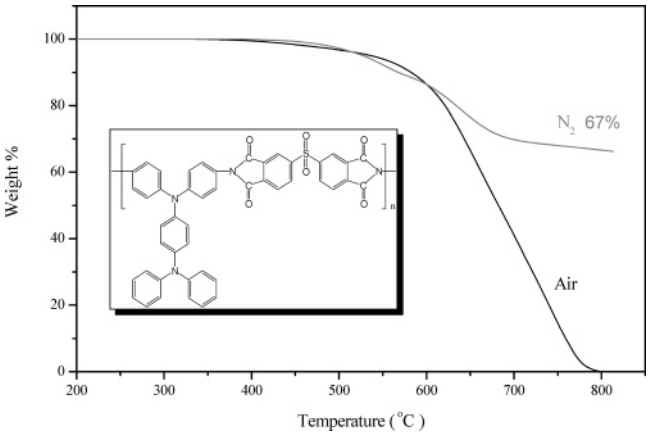

Figure 5. TGA thermograms of poly(amine-imide) **6e** at a scan rate of 20 °C/min.

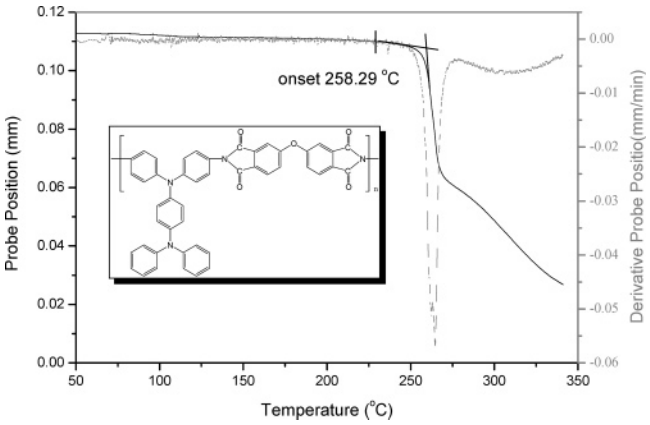

Figure 6. TMA curve of poly(amine-imide) **6d** with a heating rate of 10 °C/min.

and the onset absorption wavelength, and the results are listed in Table 5. For example, the oxidation half-wave potential for poly(amine-imide)s **6e** has been determined as 0.78 V vs Ag/AgCl. The external ferrocene/ferrocenium (Fc/Fc^+) redox standard $E_{1/2}$ is 0.50 V vs Ag/AgCl in CH_3CN. Assuming that the HOMO energy for the Fc/Fc^+ standard is 4.80 eV with respect to the zero vacuum level, the HOMO energy for poly(amine-imide)s **6e** has been evaluated to be 5.08 eV.

Electrochromic Characteristics. Electrochromism of the poly(amine-imide) thin films was monitored by a UV−vis spectrometer at different applied potentials. The electrode preparations and solution conditions were identical to those used in cyclic voltammetry. The typical electrochromic absorption spectra of poly(amine-imide)s

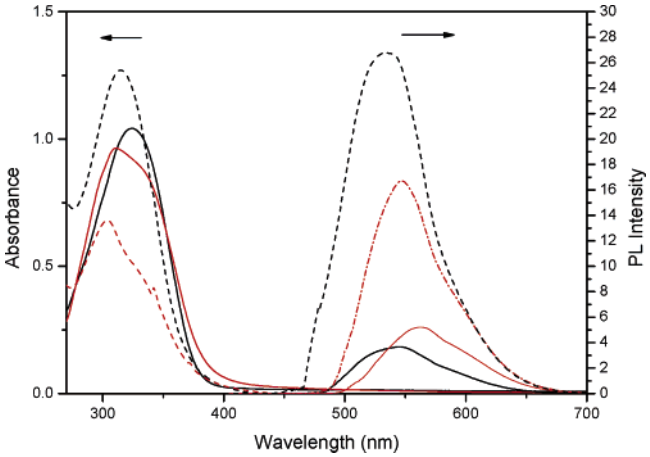

Figure 7. Absorptions and PL spectra of poly(amine-imide) **6d, 6e** (black and red solid line) and **6′d, 6′e** (black and red dash-dot line) in NMP solution.

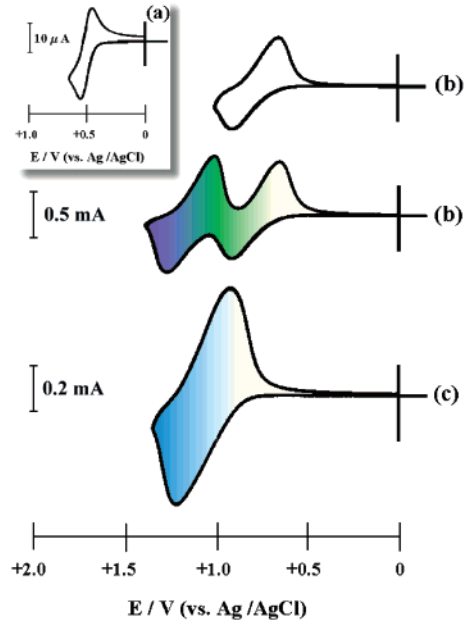

Figure 8. Cyclic voltammograms of (a) ferrocene (b) poly(amine-imide) **6e** (c) poly(amine-imide) **6′e** film onto an indium−tin oxide (ITO)-coated glass substrate in CH_3CN containing 0.1 M TBAP. Scan rate = 0.1 V/s.

6e and **6′e** are shown as Figures 9−11. When the applied potential was increased positively from 0.65 to 0.98 V, the peak of characteristic absorbance at 320 nm for poly(amine-imide) **6e** decreased gradually while two new bands grew up at 420 and 879 nm due to the first

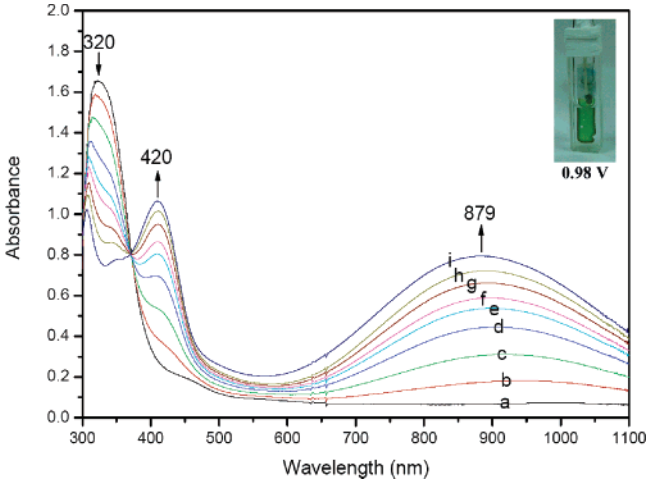

Figure 9. Electrochromic behavior of poly(amine-imide) **6e** thin film (in CH_3CN with 0.1 M TBAP as the supporting electrolyte) at (a) 0.0, (b) 0.65, (c) 0.70, (d) 0.75, (e) 0.79, (f) 0.83, (g) 0.88, (h) 0.92, and (i) 0.98 V.

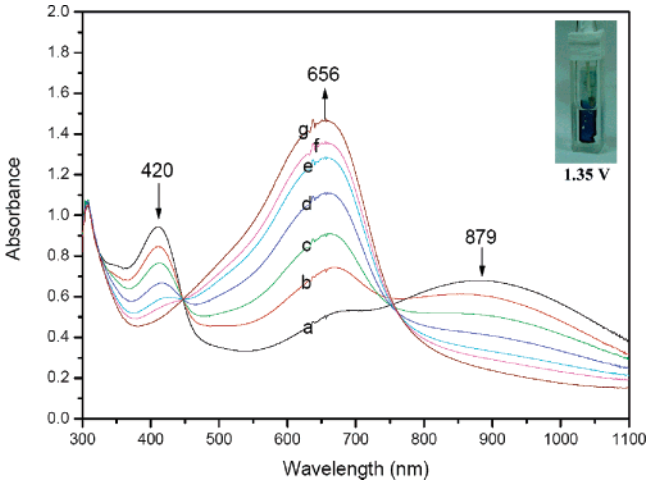

Figure 10. Electrochromic behavior of poly(amine-imide) **6e** thin film (in CH_3CN with 0.1 M TBAP as the supporting electrolyte) at (a) 1.01, (b) 1.05, (c) 1.10, (d) 1.14, (e) 1.20, (f) 1.28, and (g) 1.35 V.

electron oxidation. The new spectrum was assigned as that of the cationic radical poly(amine-imide)$^{+\bullet}$. Meanwhile, the film color turned to the green (as shown in Figure 9). When the potential was adjusted to a more positive value, corresponding to the second electron oxidation, the spectral change is shown as Figure 10. The characteristic peaks for poly(amine-imide) $^{+\bullet}$ disappeared and a new band grew at 656 nm. The new spectrum was assigned as poly(amine-imide)$^{2+}$. The film color became deep blue. The electrochromic characteristics of poly(amine-imide) **6′e** was also shown in Figure 11. When the applied potential increased positively from 0.93 to 1.30 V, the peak of characteristic absorbance at 311 nm for poly(amine-imide) **6′e** decreased gradually, while new bands grew at 390, 486, and 777 nm. The new spectrum was assigned as that of the cationic radical poly(amine-imide)$^{+\bullet}$ which appeared the complementary color of blue after oxidation.

The color-switching times were estimated by applying a potential step, and the absorbance profiles were followed (Figures 12 and 13). The switching time was defined as the time that was required to reach 90% of the full change in absorbance after switching potential. Thin films from poly(amine-imide) **6e** would require 20

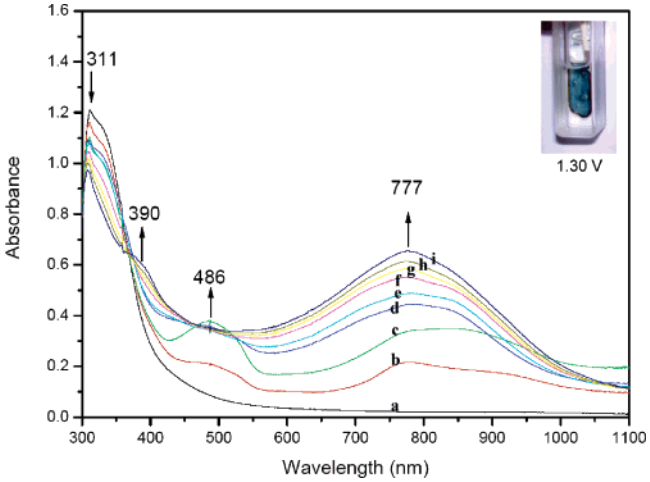

Figure 11. Electrochromic behavior of poly(amine-imide) **6′e** thin film (in CH_3CN with 0.1 M TBAP as the supporting electrolyte) at (a) 0, (b) 0.93, (c) 0.96, (d) 1.04, (e) 1.08, (f) 1.15, (g) 1.19, (h) 1.23, and (i) 1.30 V.

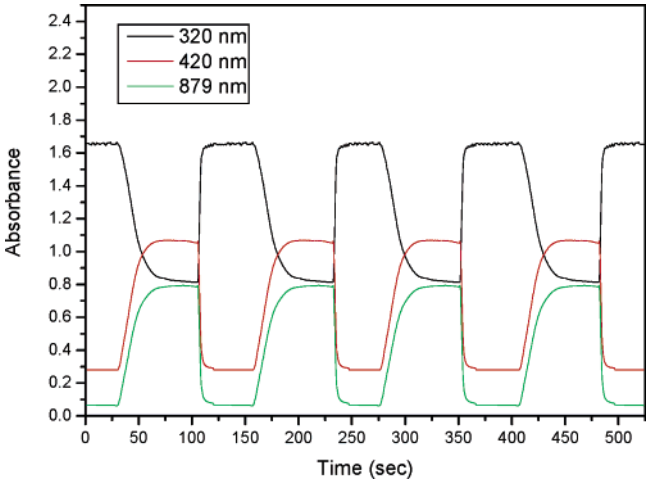

Figure 12. Potential step absorptometry of poly(amine-imide) **6e** (in CH_3CN with 0.1 M TBAP as the supporting electrolyte) by applying a potential step (0 V D 0.98 V).

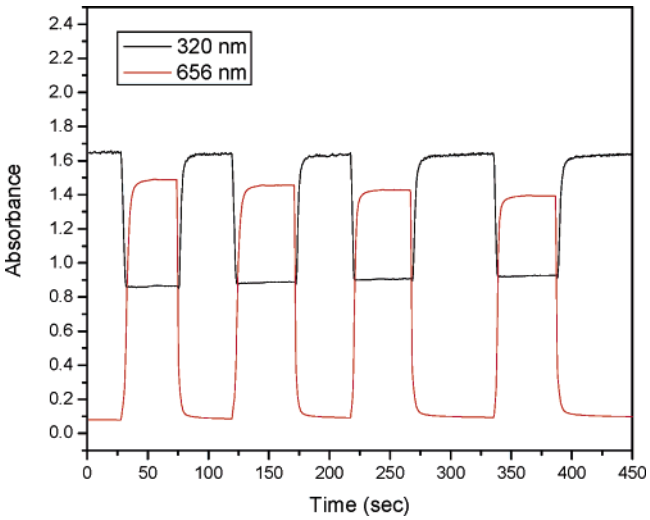

Figure 13. Potential step absorptometry of poly(amine-imide) **6e** (in CH_3CN with 0.1 M TBAP as the supporting electrolyte) by applying a potential step (0 V Δ 1.35 V).

s at 0.98 V for switching absorbance at 420 and 879 nm and 3 s for bleaching. When the potential was set at 1.35 V, thin films from poly(amine-imide) **6e** would

require almost 7 s for coloration at 656 nm and 2 s for bleaching. During five continuous cyclic scans between 0.0 and 1.35 V, the polymer films still exhibited excellent stability of electrochromic characteristics.

Conclusions

The new triphenylamine-containing aromatic diamine, *N*,*N*-bis(4-aminophenyl)-*N*′,*N*′-diphenyl-1,4-phenylenediamine (**4**) was successfully synthesized in high purity and good yields. The novel aromatic poly(amine-imide)-bearing pendent triphenylamine groups were prepared by the one-step or the two-step method starting from diamines with various aromatic tetracarboxylic dianhydrides. The introduction of the bulky, intrinsicly electron-donating triphenylamine group could decrease the HOMO energy levels and disrupt the copolanarity of aromatic units in chain packing which increases the between-chain spacing or free volume, thus enhancing solubility of the formed poly(amine-imide)s. All the poly(amine-imide)s were amorphous in nature, as evidenced by the WAXD and DSC analysis. These polymers could afford tough and flexible films with good mechanical properties and high thermal stability. All obtained poly(amine-imide)s revealed excellent stability of electrochromic characteristics, changing color from the pale yellowish neutral form to the green and blue oxidized forms when scanning potentials positively from 0.78 to 1.14 V. Thus, our novel poly(amine-imide)s have a great potential as a new type of hole-transporting and electrochromic materials due to their proper HOMO values and excellent electrochemical and thermal stability.

Acknowledgment. The authors are grateful to the National Science Council of the Republic of China for financial support of this work (Grant No. NSC 92-2216-E-260-001).

References and Notes

(1) Law, K. Y. *Chem. Rev*. **1993**, 93.
(2) Mitschke, R. H.; Bauerle, P. *J. Mater. Chem.* **2000***, 10*, 1471
(3) Forrest, S. R. *Chem. Rev*. **1997**, *97*, 1793.
(4) Marken, F.; Hayman, C. M.; Bulman Page, P. C. *Electrochem. Commun*. **2002**, *4*, 462.
(5) Marken, F.; Webster, S. D.; Bull, S. D.; Davies, S. G. *J. Electroanal. Chem*. **1997**, *437*, 209.
(6) Wadhawan, J. D.; Evans, R. G.; Banks, C. E.; Wilkins, S. J.; France, R. R.; Oldham, N. J.; Fairbanks, A. J.; Wood, B.; Walton, D. J.; Schroder, U.; Compton, R. G. *J. Phys. Chem. B* **2002**, *106*, 9619.
(7) Davies, W. B.; Svec, W. A.; Ratner, M. A.; Wasielewski, M. R. *Nature* **1998**, *396*, 60.
(8) Akcelrud, L. *Prog. Polym. Sci.* **2003**, *28*, 875.
(9) Katsuma, K.; Shirota, Y. *Adv. Mater.* **1998**, *10*, 223.
(10) Shirota, Y.; Kinoshita, M.; Noda, T.; Okumoto, K.; Ohara, T. *J. Am. Chem. Soc.* **2000**, *122*, 11021.
(11) Shirota, Y.; Okumoto, K.; Inada, H. *Synth. Met.* **2000**, *111*−*112*, 387.
(12) Giro, G.; Cocchi, M.; Lalinowski, J.; Fattori, V.; Di Macro, P.; Dembech, P.; Seconi, G. *Adv. Mater. Opt. Electron.* **2000**, *9*, 189.
(13) Thomas, K. R. J.; Lin, J. T.; Tao, Y. T.; Ko, C. W. *Chem. Mater.* **2002**, *14*, 1354.
(14) Thomas, K. R. J.; Lin, J. T.; Tao, Y. T.; Chuen, C. H. *Chem. Mater.* **2002**, *14*, 2796.
(15) Okumoto, K.; Shirota, Y. *Chem. Mater.* **2003**, *15*, 699.
(16) Lu, J.; Hlil, A. R.; Sun, Y.; Hay, A. S. *Chem. Mater.* **1999**, *11*, 2501.
(17) Ogino, K.; Kanegawa, A.; Yamaguchi, R.; Sato, H.; Kurjata, J. *Macromol. Rapid Commun.* **1999**, *20*, 103.
(18) Li, H.; Geng, Y.; Tong, S.; Tong, H.; Hua, R.; Su, G.; Wang, L.; Jing, X.; Wang, F. *J. Polym. Sci., Part A: Polym. Chem.* **2001**, *39*, 3278.
(19) Wang, X.; Nakao, M.; Ogino, K.; Sato, H.; Tan, H. *Macromol. Chem. Phys.* **2001**, *202*, 117.
(20) Behl, M.; Hattemer, E.; Brehmer, M.; Zentel, R. *Macromol. Chem. Phys.* **2002**, *203*, 503.
(21) Kim, Y.; Han, K.; Ha, C. S. *Macromolecules* **2002**, *35*, 8759.
(22) Nomura, M.; Shibasaki, Y.; Ueda, M.; Tugita, K.; Ichikawa, M.; Taniguchi, Y. *Macromolecules* **2004**, *37*, 1204.
(23) Ego, C.; Grimsdale, A. C.; Uckert, F.; Yu, G.; Srdanov, G.; Mullen, K. *Adv. Mater.* **2004**, *14*, 809.
(24) Chou, M. Y.; Leung, M. K.; Su, Y. L.; Chiang, C. L.; Lin, C. C.; Kuo, C. K.; Mou, C. Y. *Chem. Mater.* **2004**, *16*, 654.
(25) *Polyimides*; Wilson, D., Stenzenberger, H. D., Hergenrother, P. M., Eds.; Blackie: Glasgow and London, 1990.
(26) *Polyimides: Fundamentals and Applications;* Ghosh, M. K., Mittal, K. L., Eds.; Marcel Dekker: New York, 1996.
(27) Harris, F. W.; Hsu, S. L.-C. *High Perform. Polym.* **1989**, *1*, 1.
(28) Imai, Y. *React. Funct. Polym.* **1996**, *30*, 3.
(29) Hsiao, S. H.; Li, C. T. *Macromolecules* **1998**, *31*, 7213.
(30) Liou, G. S. *J. Polym. Sci., Part A: Polym. Chem.* **1998**, *36*, 1937.
(31) Eastmond, G. C.; Paprotny, J.; Irwin, R. S. *Polymer* **1999**, *40*, 469.
(32) Eastmond, G. C.; Gibas, M.; Paprotny, J. *Eur. Polym. J.* **1999**, *35*, 2097.
(33) Reddy, D. S.; Chou, C. H.; Shu, C. F.; Lee, G. H. *Polymer* **2003**, *44*, 557.
(34) Myung, B. Y.; Ahn, C. J.; Yoon, T. H. *Polymer* **2004**, *45*, 3185.
(35) Liou, G. S.; Hsiao, S. H.; Ishida, M.; Kakimoto, M.; Imai, Y. *J. Polym. Sci., Part A: Polym. Chem.* **2002**, *40*, 2810.
(36) Liou, G. S.; Hsiao, S. H.; Ishida, M.; Kakimoto, M.; Imai, Y. *J. Polym. Sci., Part A: Polym. Chem.* **2002**, *40*, 3815.
(37) Liou, G. S.; Hsiao, S. H. *J. Polym. Sci., Part A: Polym. Chem.* **2003**, *41*, 94.
(38) Hsiao, S. H.; Chen, C. W.; Liou, G. S. *J. Polym. Sci., Part A: Polym. Chem*. **2004**, *42*, 3302.
(39) Oishi, Y.; Ishida, M.; Kakimoto, M.; Imai, Y.; Kurosaki, T. *J. Polym. Sci., Part A: Polym. Chem.* **1992**, *30*, 1027.
(40) Gujadhur, R.; Venkataraman, D.; Kintigh, J. T. *Tetrahedron Lett*. **2001**, *42*, 4791.
(41) Urgaonkar, S.; Xu, J. H.; Verkade, J. G. *J. Org. Chem.* **2003**, *68*, 8416.
(42) Bergstrom, F. W.; Granara, I. M.; Erickson, V. *J. Org. Chem.* **1942**, *7*, 98.

MA048774D